33.5324.00/02/03 – Confidential

REPORT

Studies on the likelihood for caprock fracturing in the Sleipner CO_2 injection case

- A contribution to the Saline Aquifer CO_2 Storage (SACS) project

Peter Zweigel and Lars Ketil Heill

www.sintef.no

SINTEF Petroleum Research

April 2003

SINTEF

SINTEF

SINTEF Petroleumsforskning AS
SINTEF Petroleum Research

NO-7465 Trondheim

Telephone: (+47)73 59 11 00
Fax: (+47)73 59 11 02 (aut.)

Enterprise No.:
NO 936 882 331

REPORT

TITLE

Studies on the likelihood for caprock fracturing in the Sleipner CO_2 injection case – A contribution to the Saline Aquifer CO_2 Storage (SACS) project

AUTHOR(S)

Peter Zweigel and Lars Ketil Heill

CLASSIFICATION	CLIENT(S)
Confidential	Statoil, SACS consortium, NFR-KLIMATEK
REPORT NO. 33.5324.00/02/03	

REG. NO.	DATE	PROJECT MANAGER	SIGN.
2003.020	29 April 2003	Peter Zweigel	*Peter Zweigel*
NO. OF PAGES	NO. OF APPENDICES	LINE MANAGER	SIGN.
27	1	Torleif Holt	*Torleif Holt*

SUMMARY

Injection of CO_2 into the Utsira Sand at the Sleipner field may increase formation pressure and impose buoyancy forces onto the seal formation. This study assesses the likelihood for injection-induced fracturing of the seal rock at the Sleipner CO_2 storage site.

A literature survey on the present day subsurface stress conditions in the area summarizes published results from borehole breakout analyses, focal mechanism analyses, stress inversions of leak-off tests, integrated stress measurements and overcoring experiments, and utilises data in the World Stress Map database. Published data indicate small deviatoric stresses in the area of interest and therefore a small likelihood only for induced fracturing or reactivation of existing faults.

Rock mechanical calculations address the Sleipner case by two methods: (a) treating the elongate, domal trap as a segment of a horizontal well, applying well stability calculation procedures, and (b) using finite element analysis. Both methods indicate that it is unlikely that the cap of the trap will fracture due to the injected CO_2.

KEYWORDS ENGLISH	KEYWORDS NORWEGIAN
Carbon dioxide storage	Karbondioksidlagring
North Sea	Nordsjøen
Sleipner field	Sleipnerfeltet
Recent stress field	Nåværende stressfelt
Caprock failure	Takbergartssvikt

Table of Contents

1. Introduction

At the Sleipner field in the North Sea, CO_2 is separated from natural gas and stored in the underground at a rate of approximately 1 million ton CO_2 per year. CO_2 is injected near the base of the highly porous and highly permeable Utsira Sand, through which it rises buoyancy-driven upwards towards its seal, the shales of the Nordland Group. Thin shale-layers in the Utsira Sand provide migration barriers and baffles, but most of the injected CO_2 is expected to ultimately accumulate beneath the top seal of the formation.

The density difference between CO_2 and formation water at reservoir conditions causes a pressure acting on the seal. This pressure may theoretically induce fracturing of the seal or reactivate potentially existing fractures and faults. Since these processes may compromise reservoir safety, their likelihood was investigated in the present study.

This report presents results of two largely separate studies:

a) a literature survey on the present-day stress field in the Sleipner area and its surroundings (North Sea), and
b) rock mechanical calculations to assess the likelihood for induced fracturing.

The literature study (Chapter 2) was carried out by Peter Zweigel and was largely done in 1999/2000 with a minor update to include some newer literature of relevance in 2002. The rock mechanical calculations (Chapter 3) were carried out by Lars Ketil Heill in 2000. The calculations do consequently not include parameters made available later in the SACS project. They assume especially a brittle seal lithology, whereas inspection of a seal core acquired in 2002 indicates a weak rock with considerable plasticity. However, this rock behaviour makes fracturing even less likely than calculated.

2. Recent stress field in the North Sea – a literature study

2.1 Data types and data sources

Stress orientations (mainly the orientation of the maximum horizontal stress, S_H) in the North Sea and the adjacent parts of Scandinavia have been interpreted and publicly reported from analysis of borehole breakouts, focal mechanism analysis of earthquakes, and by overcoring experiments. Relative magnitudes of the maximum (S_H) and minimum (S_h) horizontal stresses have been determined by inversion of leak-off tests, whereas absolute magnitudes and orientations of the three principal stress axes (and, thus, also S_H, S_h, and the vertical stress S_V) stem from 'integrated stress measurements' and overcoring experiments.

Borehole breakout analyses or analyses of drilling-induced tensile fractures from image logs were carried out for a large number of wells in the northern North Sea, and data is documented in, e.g., Spann et al. (1991), Cowgill et al. (1995), Fejerskov et al. (1995), Fejerskov (1996), Goelke (1996), Goelke & Brudy (1996), Brudy (1998), Fejerskov & Bratli (1998), Wiprut & Zoback (1998), Fejerskov et al. (2000), Grollimund et al. (2001) and Brudy & Kjørholt (2001). These data are generally from offshore, and some data-points are from close to the Sleipner area. Since this type of data is derived from drilling depths (most from between 1000m to 4000m TVDss) they are from depths and partly from rocks with mechanical properties similar to those of interest. They do, however, provide no information about stress magnitudes. Grollimund et al. (2001) and Brudy & Kjørholt (2001) stress the limitations of the borehole breakout analysis method, including the effect of key seating in cases of boreholes deviating from the vertical.

Focal mechanism analyses for earthquakes with foci in the northern North Sea and the adjacent Scandinavian mainland have been documented in, e.g., Gregersen et al. (1991), Gregersen (1992), Fejerskov et al. (1995), Lindholm et al. (1995a & b, 2000), Fejerskov (1996). There exist no data from close to the Sleipner area. A disadvantage of focal mechanism results is that they relate mostly to events from depths far below the depth of interest in the Sleipner area (i.e. from the basement instead of the sedimentary basin fill), and they may, thus, represent a strongly different stress field.

Stress inversion of leak-off tests from wells of the northern North Sea has only rarely been published, Aadnøy & Berland (1995) and Jørgensen & Bratli (1995) being the only public data sources found by us. Jørgensen & Bratli (1995) present ratios of S_H vs. S_h. However, since the results reported there are from the northernmost part of the North Sea (block 34) where the stress pattern indicates perturbations relative to the overall regional stress field (see below), they may not be representative for the Sleipner area some 250 km of it.

'Integrated stress measurements' (Zoback et al. 1993; Brudy et al. 1997) provide orientations and magnitudes of all three principal stress axes. Data from the North Sea are so far only documented in Brudy (1998), Wiprut & Zoback (1998), and Grollimund & Zoback (2000). Brudy does not provide the location of the studied wells. The other

data are from the Visund field (block 34), thus, the same restrictions for applicability as for the stress inversion data are valid.

Overcoring experiments provide the full stress tensor, i.e. orientations and absolute magnitudes of the principal stress axes. Data from Scandinavia are documented in, e.g. Stephansson et al. (1991), Fejerskov (1996), and in sources for the World Stress Map data base (Mueller et al. 1997, see below). All data are, however, from the mainland and thus from a considerable distance to the Sleipner area. Since the data from south-western Norway are from basement units, they may not be representative for the stress field in the sedimentary cover units of the adjacent North Sea.

Additional data derived by various methods is contained in the **World Stress Map** data base (Release 1997-1, Mueller et al. 1997). We used in our interpretation predominantly data from this source, supplemented by some data from the references quoted above. We did this, because the data in the World Stress Map (WSM) data base have already undergone a quality assessment. For an explanation of the quality ranking scheme used, refer to Mueller et al. (1997). Principal aspects of quality ranking were discussed with the former WSM co-ordinator, Dr. B. Sperner.

2.2 The orientation of the stress field

Large parts of Western Europe are dominated by approximately NW-striking maximum horizontal stress axes (S_H) (Zoback 1992). World Stress Map (WSM, release 1997-1, Mueller et al. 1997) data from the North Sea show this preference, too, which is stronger when only data sets of the three highest quality levels A to C (out of A to E) are used (Figure 2.1, Figure 2.2a&b, Table 2.1). The same preference is apparent, when selecting the WSM97-1 data for the southern part of the northern North Sea (Figure 2.2c&d). There is, however, considerable variance in strike between individual S_H determinations. This is in line with the reported general tendency of progressively stronger alignment of S_H axes when following the western margin of Scandinavia from South (Central North Sea) to North (Barents Sea) (e.g. Gregersen et al. 1991, Fejerskov et al. 1995, 2000).

For the northern part of the North Sea (north of Sleipner), Brudy & Kjørholt (2001) and Grollimund et al. (2001) document high-quality S_H orientation data which consistently show a regionally varying strike from 100º west of the Viking Graben to 80º towards the Norwegian coast. For the central part of the North Sea (south of Sleipner), Grollimund et al. (2001) report varying S_H strike directions with a tendency towards NW/NNW, whereas the analysis of Brudy (2001) yielded mainly E-W-striking S_H. Both these studies analysed wells in the Sleipner area but were not able to deduce S_H from the well data.

For the direct neighbourhood of the Sleipner area, the WSM97-1 data show the preference of a NW-strike only in low quality data (Figure 2.2e), whereas the single high quality entry contains a S_H-strike of 86° (Figure 2.2f). Goelke (1996; also included in Mueller et al. 1997) reports the borehole breakout analysis from closest to the injection site (his data are from well 15/9-18, but from a depth range 3125-3225), which

is a 113°-striking S_H of quality D. Cowgill et al. (1995) present results of three wells in the close neighbourhood of the Sleipner area graphically, where strike of S_H ranges from 23° over 85° to 155°; quality ranking and depth intervals are not provided.

In summary, there seems to be considerable variation in the orientation of S_H in and around the Sleipner area (Figure 2.3), in spite of the clear regional dominance of a NW-trending maximum horizontal compression axis. Some variation between values from different wells in close neighbourhood might in general be due to differences in depth of the interpreted intervals (cf., e.g., the considerable azimuth changes as a function of depth in well 31/2-4 reported in Goelke 1996). Where depth information is available for the data from the Sleipner area, the interpreted intervals are from 2750 to 3400 m drilling depth, i.e. from a relatively small depth range and from rocks that are not separated from each other by decoupling horizons. Depth differences should, therefore, play only a minor role.

The observed azimuth variation may, however, be due to small differences in magnitude between S_H and S_h, which would allow for considerable changes in their orientation as a consequence of local influences (such as topographic gradients, spatial distribution of rock mechanical properties). Possible reasons for such perturbations in the Sleipner area can be speculated to be, e. g., due to its position at the northern fringe of the underlying, stress-decoupling Permian salt or due to its tectonic position close to the triple junction of the Jurassic rift system.

Table 2.1 Selection criteria, number of data entries in selections, and mean azimuths for subgroups of the World Stress Map database (Release 1997-1, Mueller et al. 1997). Azimuths of data are graphically displayed in Figure 2.2. Quality levels range from A to E, A being highest quality rank and E lowest.

Data set	Latitude	Longitude	Quality	Number	Mean azimuth
NS-sel1	54.5N - 62N	4W - 8 E	A-E	171	133
NS-sel2	54.5N - 62N	4W - 8 E	A-C	60	118
NS-sel3	57.5N - 60N	1W - 5E	A-E	52	124
NS-sel4	57.5N - 60N	1W - 5E	A-C	12	122
NS-sel5	58N - 59N	0.5E - 3E	A-E	7	115
NS-sel6	58N - 59N	0.5E - 3E	A-C	1	68

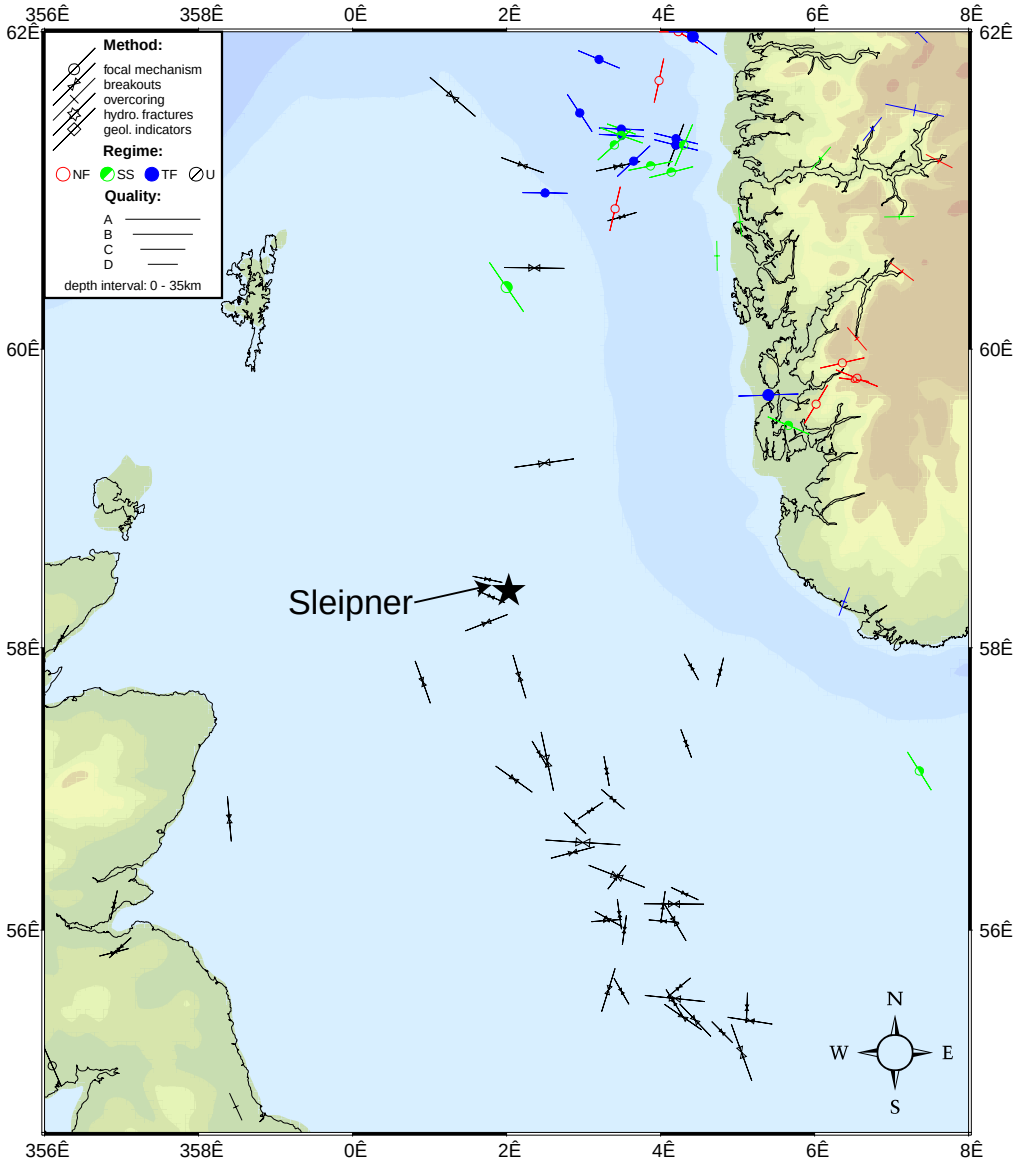

Figure 2.1 *Orientation of maximum horizontal stress axes (S_H) in the Central and Northern North Sea according to the World Stress Map database (Release 1997-1; Mueller et al. 1997). The data points are marked according to their quality, the stress regime, and the method by which the stress orientation was determined. Map (a, this page) contains data of quality classes A to D and map (b, next page) only data of the higher quality classes A to C. The figure was prepared by B. Sperner, Karlsruhe.*

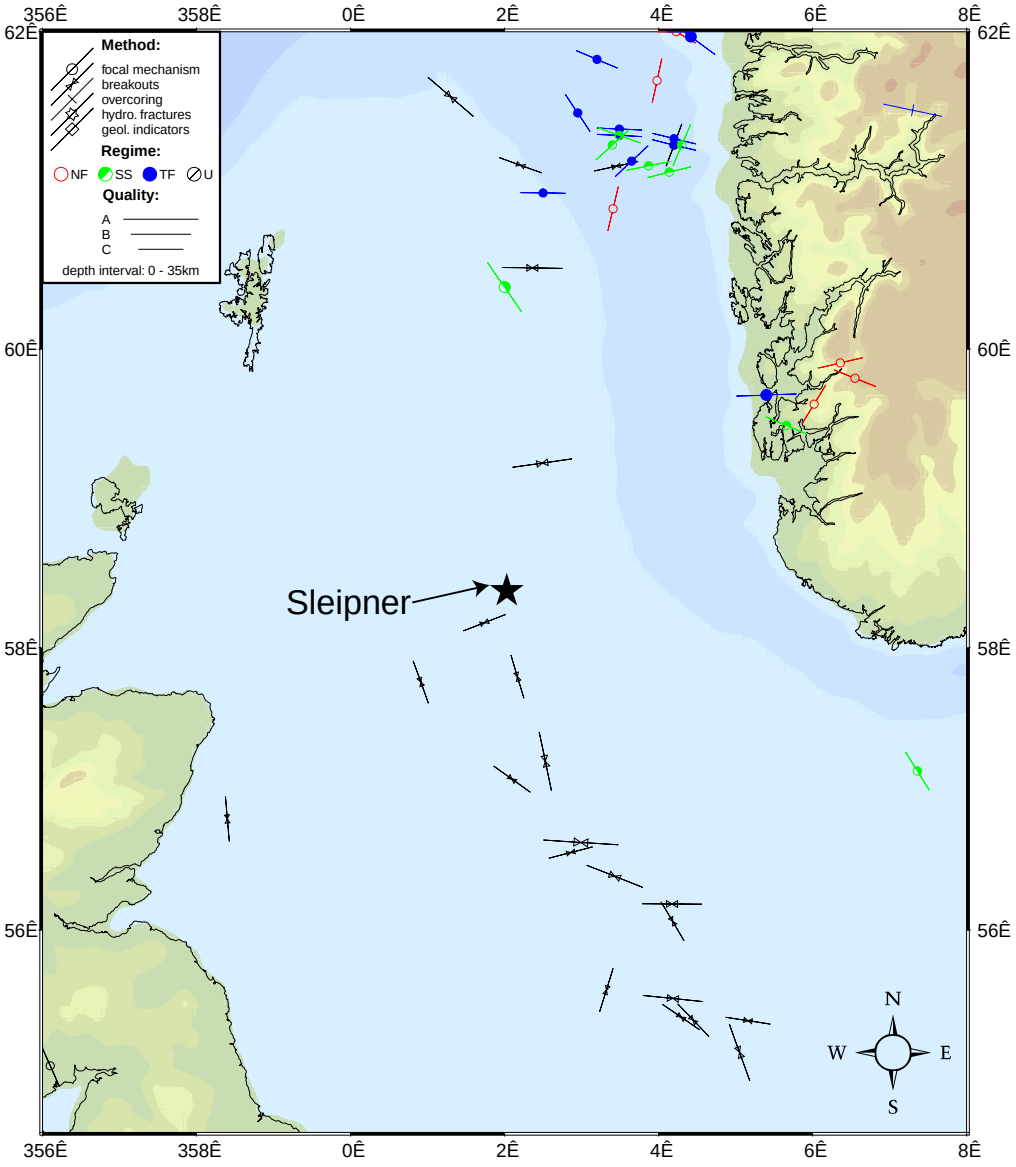

Figure 2.1b: Figure text on previous page

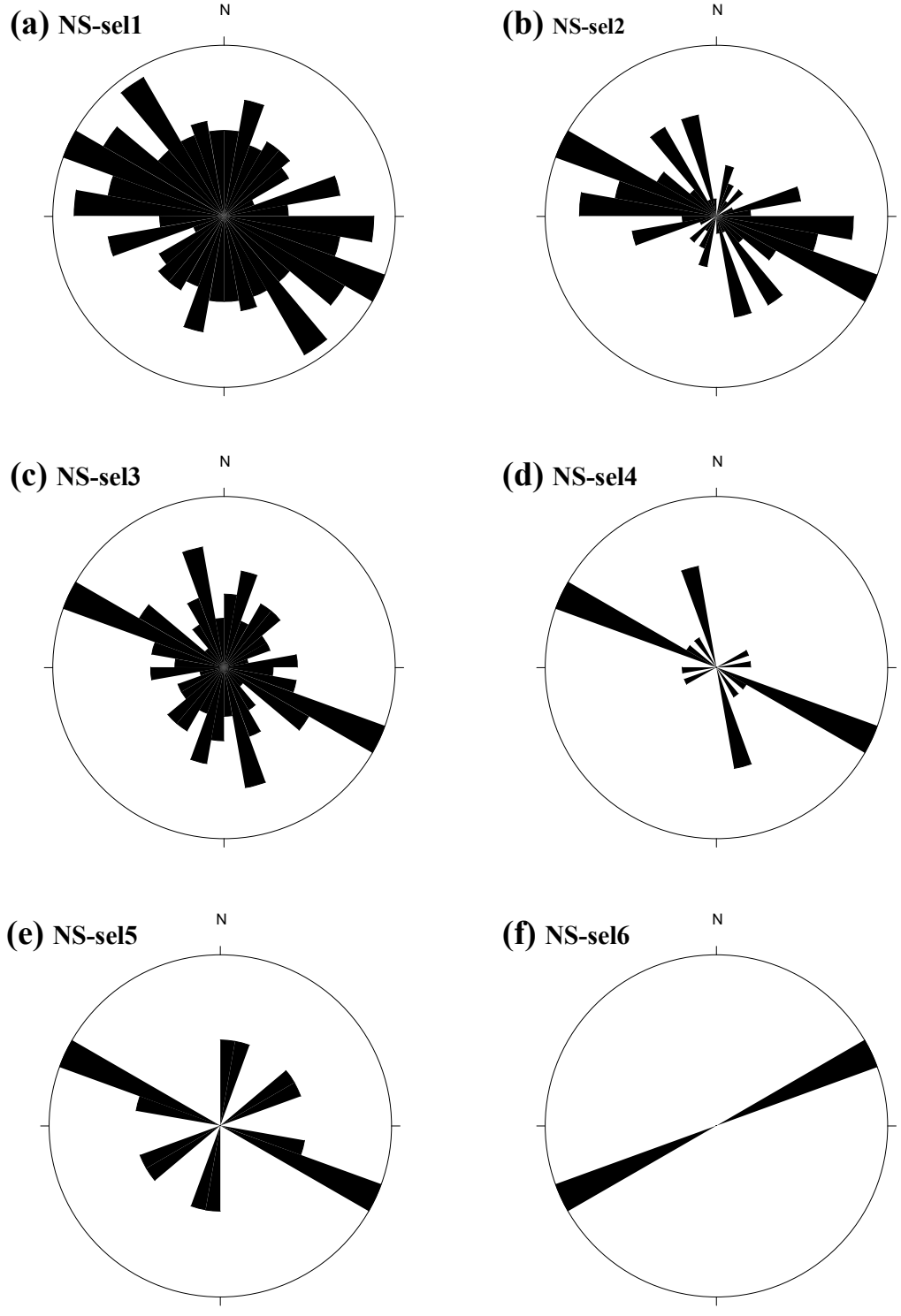

Figure 2.2 Rose diagrams illustrating the trend (azimuth) of maximum horizontal compression axes (S_H) in the Central and Northern North Sea (cf. Table 2.1) as derived from regional selections of the World Stress Map database (Release 1997-1, Mueller et al. 1997). The selections cover progressively smaller areas from top to bottom, focussing towards the Sleipner area. The left and right columns contain data of quality ranks A to E and A to C, respectively; A is highest quality rank and E lowest. Refer to Table 2.1 for selection criteria, data size and mean azimuths.

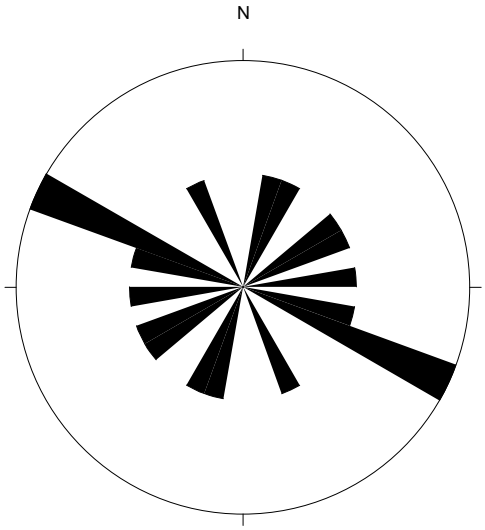

Figure 2.3 Rose diagram illustrating the trend (azimuth) of maximum horizontal compression axes (S_H) determined from borehole break-out analyses of wells in, or close to, the Sleipner area. Data are from Cowgill et al. (1995) and from other sources listed in Mueller et al. (1997). The WSM data (Mueller et al., 1997) are qualities A to D and from the same area as data-set NS-sel6 (Table 2.1). A large scatter of the data (N = 9) is evident.

2.3 Stress regime and magnitude of differential stress

Zoback (1992) summarised the then available recent stress field data which indicated a dominating strike-slip (SS; $S_V = S_2$, for $S_1 > S_2 > S_3$ and compressive stresses being positive) regime with NW-striking S_H. The presently available WSM data (Mueller et al. 1997) confirm this interpretation (Figure 2.4): strike-slip data sets dominate and there are less normal faulting data sets (NF; $S_V = S_1$) then thrust faulting data sets (TF; $S_V = S_3$), especially when only high quality data sets are considered. This majority of horizontally compressive over vertically compressive data sets persists when oblique normal faulting (NS) and oblique thrust faulting (TS) data are included (Figure 2.4).

Determinations of relative and absolute principal stress magnitudes exist from the northernmost part of the North Sea (block 34) and onshore South-west Norway. Jørgensen & Bratli (1995) report small ratios between S_H and S_h from stress inversions of leak-off rests in the Tampen area, S_H/S_h ranging from 1.04 to a maximum of 1.20, with a mean of 1.09 and a standard deviation of 0.045. With the exception of one case, S_H and S_h were always smaller than S_V, i.e. a normal faulting to strike-slip stress regime. These small ratios indicate a nearly isotropic stress field in the horizontal, which is in line with the large scatter of azimuths of S_H that Jørgensen & Bratli (1995) report, too. S_1/S_3 (i.e. mainly S_V/S_h) ranges from 1.10 to 1.33, with a mean of 1.20 and a standard deviation of 0.11.

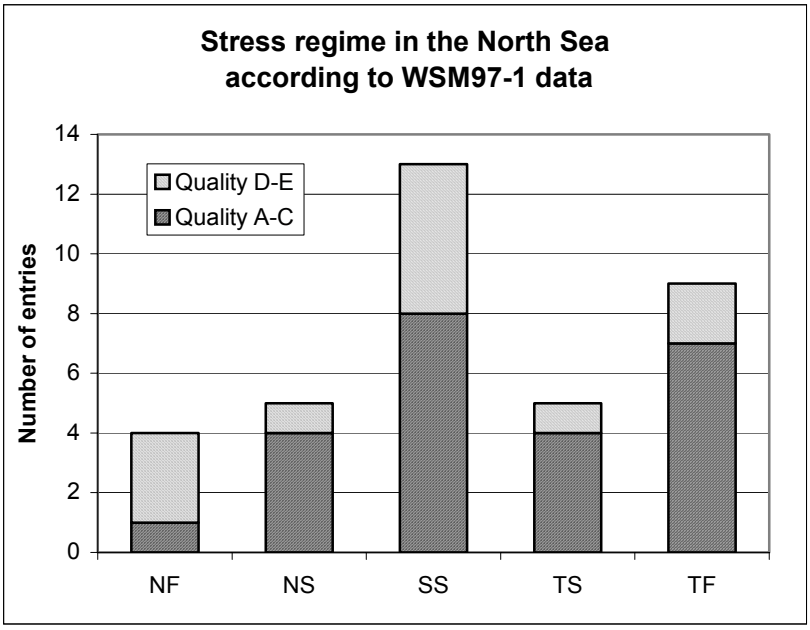

Figure 2.4 *Frequency distribution of stress regimes in the Central and Northern North Sea as derived from a regional selection of the World Stress Map database (Release 1997-1, Mueller et al. 1997). The selection is limited to 54.5° – 62° N and 4° W to 8° E. Note that the majority of data in that area is from borehole breakout analyses, which do not allow for determination of the stress regime. NF: Normal faulting regime; NS: Oblique normal faulting regime; SS: Strike-slip regime; TS: Oblique thrust faulting regime; TF: Thrust faulting regime (further explanations: see text).*

Wiprut & Zoback (1998) report stress magnitudes from application of the 'Integrated Stress Measurement Strategy' to well data from the Visund field (block 34). S_H is there always considerably larger than S_V, which in turn is slightly larger than S_h, i.e. the stress regime is most likely strike slip. Deviatoric stresses ($S_1 - S_3$, i.e. here: $S_H - S_h$) range from 16.6 MPa to 26.5 MPa (with partly large error brackets of up to 23 MPa!) with corresponding S_H/S_h ratios between 1.28 and 1.37. Wiprut and Zoback (1998) derive accordingly for the Visund field area a constant azimuth of S_H of ca 100°. Similarly, Brudy (1998) reports deviatoric stress magnitudes in a strike-slip regime (S_H-S_h) that range from 12 MPa to at least 26 MPa, and corresponding S_H/S_h ratios that range from 1.31 to at least 1.49.

The differences between the studies of Jørgensen & Bratli (1995) and Wiprut & Zoback (1998) are striking. However, we are not able to provide an explanation for it, especially since both, methodology and data used, are only scarcely documented. The extrapolation of results from the northernmost North Sea to the Sleipner area may not be fully appropriate, regarding the distance (ca. 250 km) and the differences in tectonic setting (transition between the Viking Graben system and the Møre-Trøndelag fault

zone in the North (Gabrielsen et al. 1999) and southern termination of the Viking Graben at a former triple junction in the South (Underhill & Partington 1993)). That both, Brudy & Kjørholt (2001) and Grollimund et al. (2001) were not able to detect borehole breakouts or drilling-induced tensile fractures (with one low quality exception in well 15/9-A15) in wells from the Sleipner area, may signify small differential stresses there. Grollimund et al. (2001) graphically present regional data from leak-off tests compared to calculated vertical stress from integrated density logs. They show for a depth of 1500 m in the Sleipner area a ratio of S_3 / S_V close to 1, i.e. either a strike-slip or reverse (thrust) faulting regime. They report further that pore pressure at this depth is hydrostatic in the Sleipner area.

Full stress tensors have been determined by overcoring experiments onshore Norway, and data are documented in various sources to the World Stress map data base (Mueller et al. 1997) and in, e.g., Fejerskov (1996). These experiments yield mainly relatively low deviatoric stresses (Figure 2.5), with a few peaks up to 42 MPa. As a rough quality control, we plotted the magnitude of S_V (in the case of Fejerskov 1996 the stress value of that axis which is closest to a vertical position) against depth (Figure 2.6), which should yield a roughly linear relationship in the case of S_V being $S_{lithostatic}$. As Figure 2.6 shows, such a linear relationship exists, with a few deviating data points such as the one having the large deviatoric stress of 42 MPa, which we do, therefore, discard as being an interpretation error. However, the slope of the regression line corresponds to an unrealistically high rock density of 4250 kg/m^3. Most measurements are from shallow depths and from gneissic-granitic basement rocks, such that a density of less than 3000 kg/m^3 would be expected.

The applicability of the overcoring results to the Sleipner area is questionable. They are from stations which are minimum 250 km away from the Sleipner area. These stations are situated in the basement, that has different rock mechanical properties, and that, thus, possibly contains a different stress field, than the sedimentary basin fill of the Northern North Sea. Moreover, they are from a region with large topographic gradients which will influence the orientation and magnitude of the principal stress axes.

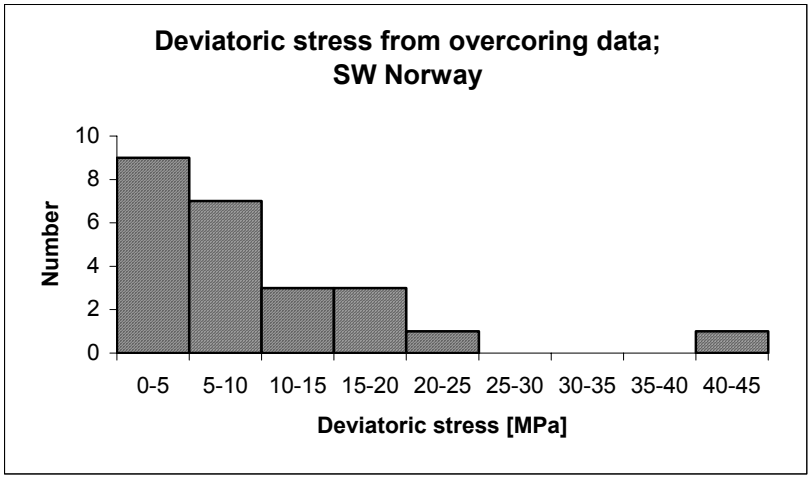

Figure 2.5 *Frequency distribution of deviatoric stress magnitudes (difference between maximum and minimum principal stress) determined by overcoring at sites from south-western Norway. Data are from World Stress Map database (Release 1997-1, Mueller et al. 1997; data south of 62° N, west of 8° E, N = 11) and from Fejerskov (1996; data south of 61° N and 7° N, N = 13).*

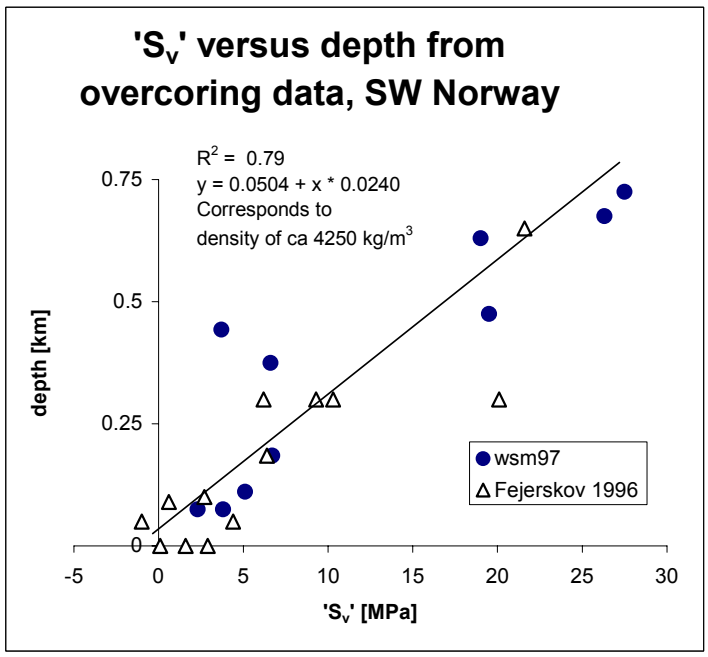

Figure 2.6 *Magnitude of principal stress axis closest to vertical position (S_1 in case of NF and NS regime, S_2 in case of SS, S_3 in case of TF and TS) versus depth of the interval analysed by overcoring. Note that the data show a good regression, but the resulting slope corresponds to a unrealistically high density of 4250 kg/m^3, when assuming the vertical stress to be lithostatic. Data sources: see text to Figure 2.5.*

2.4 Discussion

The direct applicability of existing deviatoric stress determinations from the northern North Sea and the adjacent onshore areas of south-western Norway to the Sleipner area is questionable because they are from regions far away, in different tectonic position and from different depth. The large variability of S_H azimuths in the Sleipner area suggests however that nearly isotropic conditions may prevail there.

The stress field in the northern North Sea has been modelled by finite element modelling (Goelke 1996) and distinct element modelling (commissioned by SINTEF Petroleum Research and documented in: Pascal & Gabrielsen 1999, Pascal et al. 1999, Pascal & Gabrielsen 2001). Goelke modelled the stress field for whole Europe. All his models yield a NW-oriented S_H for the northern North Sea, but in his most sophisticated model, S_H and S_h are relatively similar in magnitude.

Our commissioned distinct element model (Pascal & Gabrielsen 1999, 2001, Pascal et al. 1999) focussed on the mid Norwegian margin and the northern North Sea and did not incorporate topography effects. It predicts WNW-oriented S_H in the Sleipner area, and S_H and S_h being of similar magnitude. This model attributes the low magnitude of deviatoric stresses in the northern North Sea to a 'shielding' effect of the mechanically weak Møre-Trøndelag Fault Zone and its southwestern continuation, which protects the area south of it against ridge-push forces from the Norwegian-Greenland Sea. This shield effect and its efficacy depend only on the fault zone rheology, which – as Pascal & Gabrielsen (2001) state - is the most unconstrained parameter in their model. The model does not provide absolute stress magnitudes and is restricted to stresses and movements in map view.

We do, in conclusion, not expect the existence of large deviatoric stresses in the Sleipner area at present. This inference may also be valid for the time since deposition of the Nordland Shales, forming the cap rock of the Utsira Sand. These shales were deposited since ca. 3 Myr (Eidvin et al. 1999). Increased subsidence in the North Sea during Pliocene and Quaternary (e.g. Wood 1981, Gradstein et al. 1994) has been attributed to increased tectonic compression (e.g. Kooi et al. 1991) affecting large parts of the North Atlantic region (Cloething et al. 1990). Cloething et al. (1992), however, argue that this phase of increased compressive stress started at ca. 15 Myr, reaching its maximum at ca. 5 Myr and continuing to the present. Tectonic compressive stresses since deposition of the Nordland Shales (3 Myr to present) seem, thus, not to have changed much, or maybe to have decreased.

Further events that could have affected the regional stress field, are the glaciations and deglaciations of the near past (see e.g. Grollimund et al. 2001). We are not able to assess the importance of these changes for the magnitude of deviatoric stresses and, thus, for the likelihood of fracturing of the Nordland Shales. These rocks are, however, still largely only weakly consolidated, and consolidation was surely less in the past. We expect them, thus, rather to have reacted plastically.

A possible other, non-tectonic cause for fracturing of the Nordland Shales might be volume-loss which was not compensated by vertical compaction. Polygonal fracture

systems in the North Sea have been documented during the last few years and have been interpreted to be due to such volume loss (see, e.g. Cartwright & Lonergan 1996). This mechanism can not yet be excluded for the Nordland Shales. However, a recent study (Dewhurst et al. 1999) suggests that the smectite content of shales controls their likelihood to exhibit polygonal fractures. The Nordland Shales contain relatively minor smectite in the Sleipner area (up to 16%, but mainly below 10% according to Lothe & Zweigel 1999 and Bøe & Zweigel 2001), and are, thus, less likely to contain polygonal fractures.

3. Rock mechanical calculations of fracture likelihood

3.1 Introduction

This chapter contains numerical assessments of possible rock mechanical failure of the Utsira sand cap rock as CO_2 is injected into the sand formation 160 meters below the sand/cap rock interface. Conditions of the calculations are approximated to those of the Sleipner CO_2-injection case, however, the geometry of the setting is strongly simplified and several parameters had to be assumed due to lack of relevant input data.

3.2 Parameters

The assessments are based on mechanical parameters from log data and historical data, data from simulations of CO_2 transport and a basic description of the cap rock geometry. We consider brittle, shear failure; since the cap rock consists of shale, and not clay, we do not consider plastic failure.

Rock mechanical parameters for the cap rock shale are not available from tests on core samples. Values are tabulated in the literature (Fjær et al. 1992) or can be assumed. Here, we have used those of Table 3.1.

Table 3.1 Rock mechanical parameters used in the calculations.

Density	$\rho =$	2.35	g/cm^3	(Weak North Sea Shale)
Young's modulus	$E =$	1	GPa	(Weak North Sea Shale)
Poisson's ratio	$\nu =$	0.17		(assumed)
Unconfined compressive strength	$C_0 =$	6	MPa	(Weak North Sea Shale)
Tensile strength	$T_0 =$	0	MPa	(assumed)
Failure angle	$\beta =$	45°		(assumed)
Biot constant	$\alpha =$	1		(assumed)

Stresses and pressures: From a nearby well log (EXLOG Drillbyte EAP: OBG Data, well path 15/9-C-2H), the stresses and pressures in Table 3.2 were extracted. Note that the sand/cap rock interface is at about 830 mTVD (TVD=True Vertical Depth), corresponding to about 880 mMD (MD=measured depth, along the inclined well's trajectory). Hence, 870 mMD is in the cap rock shale while 890 mMD is in the sand formation.

Table 3.2 Stresses and pressures from well 15/9-C-2H.

Vertical stress	$\sigma_v =$	16.1	MPa	(at 870 mMD)
Horizontal stress	$\sigma_h =$	10.1	MPa	(at 870 mMD)
Cap rock pore pressure	$p_{f,c} =$	8.58	MPa	(at 870 mMD)
Sand pore pressure	$p_{f,s} =$	8.75	MPa	(at 890 mMD)

Geometry: The shallow anticline trap above the CO_2 injection point has a dip of 12.5 m and a radius from centre to spill point of approximately 800 m (Lothe & Zweigel,

1999) We adapt the same dimensions in our assessments below. In the same report, simulations of CO_2 transport from the injection point up to the cap rock trap were performed with and without a number of thin horizontal impermeable shale layers in the sand. The thin shale layers will retain much of the CO_2 and dramatically slow down the buoyancy-driven (the permeability is large, about 3 Darcy) transport up towards the sealing cap rock, so we concentrate on the conservative homogeneous sand case without internal shale layers. The transport modelling then predicted a final (i.e. at the point when CO_2 would spill out of the injection trap to other traps to the north, west or south) CO_2 distribution below the trap with a maximum thickness of 20 m (at the centre), thinning to zero at the trap perimeter. Of these 20 m, 12.5 m is due to the topography of the seal, while 7.5 m is due to a down-dip cone centred around where the CO_2 reaches the gas cap.

Density difference: At formation pressures (about 8.5 MPa, Table 3.2), the density difference between brine and gas is about 300 kg/m^3 for pure CO_2, or about 370 kg/m^3 with 2.5% methane (E. Lindeberg, pers. comm.). Assuming overpressures of about 2 MPa, as indicated by data from the Sleipner area with formation pressures about 10.7 MPa at 850 mTVD (Holloway et al. 2000, their tables 1.3 and 1.4) the maximum pressure difference is still well below 400 kg/m^3. Hence, still conservative we adopt 400 kg/m^3 as the upper limit on the brine/CO_2 pressure difference in our region of interest.

3.3 Initial evaluation

If we assume a CO_2 column with a height of 20 m fully displacing the original brine, a brine/gas pressure difference of 400 kg/m^3 corresponds to a maximum pressure increase of $\Delta p_{max} = 0.08$ MPa at the base of the cap rock due to the buoyancy of the pore fluid. Comparing this to the magnitude of the stresses and pressures in Table 3.2, it seems very unlikely that the presence of the injected CO_2 could possibly have a fatal effect on the cap rock integrity: there are two orders of magnitude difference.

3.4 Simple modelling: The dome as part of an imaginary horizontal well

The risk of cap rock failure can be assessed using a established methods from well stability analyses if the dome (i.e. the cap rock anticline trap) is modelled as a small part of a huge imaginary horizontal well (Figure 3.1) with well pressure given by the CO_2 pressure.

Since the height of the dome is only 12.5 and the width 1600 m, the radius of the imaginary well is necessarily huge: about 43 km. The dome segment of the well perimeter corresponds to an angle of about 2 degrees. We make the conservative simplification of assuming a constant "well pressure" in the dome,

$$p_w = p_{f,s} + \Delta p_{max} = (8.75 + 0.08) \text{ MPa} = 8.83 \text{ MPa}.$$

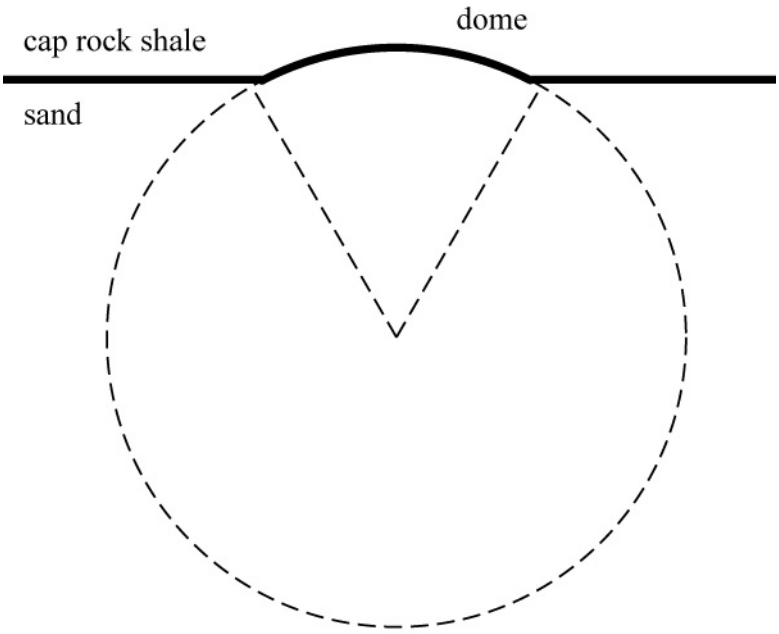

Figure 3.1 Dome as part of horizontal well.

Intuitively, we would not expect large shear stresses along the shale/sand interface for such a flat dome. Nevertheless, using the machinery of well stability analysis in Fjær et al (1992) we find that the "well pressure" would have to be larger than 12.1 MPa to induce shear failure in the impermeable cap rock shale at the top of the "well" (i.e. for $\theta \approx 0°$ in Fjær et al 1992).

Tensile failure by vertical hydraulic fracturing could happen if the "well pressure" grows large enough to make the stress along the dome surface negative, i.e. larger than $2\,\sigma_h - \alpha\, p_{f,c} + T_0 = 11.7$ MPa in this model.

Thus, with failure pressures of 11.7 and 12.1 MPa, the CO_2 column would have to be 740 to 840 m high to induce failure, while the injection point is only 160 m below the cap.

3.5 Finite element modelling

A simplified FEM modelling using the VISAGE system was carried out, using the rock mechanical parameters listed in Table 3.3. A steady-state plane strain analysis was performed assuming axial symmetry about the centre of the dome. See Figure 3.2 for details on the FEM model.

Table 3.3 Rock mechanical parameters used in the FEM modelling. Values are assumed.

Shale region			
Young's modulus	E =	1	GPa
Poisson's ratio	ν =	0.17	
Rock density	ρ_{shale} =	2.0	g/cm^3
Fluid density	$\rho_{shale,f}$ =	1.0	g/cm^3
Shear modulus	G =	5	GPa
Cohesion	S_0 =	4	MPa
Friction angle	ϕ =	45°	

Sand region w/gas			
Young's modulus	E =	2	GPa
Poisson's ratio	ν =	0.18	
Rock density	ρ_{gas} =	1.9	g/cm^3
Fluid density	$\rho_{gas,f}$ =	0.6	g/cm^3
Shear modulus	G =	5	GPa
Cohesion	S_0 =	4	MPa
Friction angle	ϕ =	37°	

Sand region			
Young's modulus	E =	2	GPa
Poisson's ratio	ν =	0.18	
Rock density	ρ_{sand} =	1.9	g/cm^3
Fluid density	$\rho_{sand,f}$ =	1.0	g/cm^3
Shear modulus	G =	5	GPa
Cohesion	S_0 =	4	MPa
Friction angle	ϕ =	37°	

The simulation does not result in Mohr-Coulomb failure anywhere: See Figure 3.3 and Figure 3.4 for more detailed presentations of the FEM modelling results.

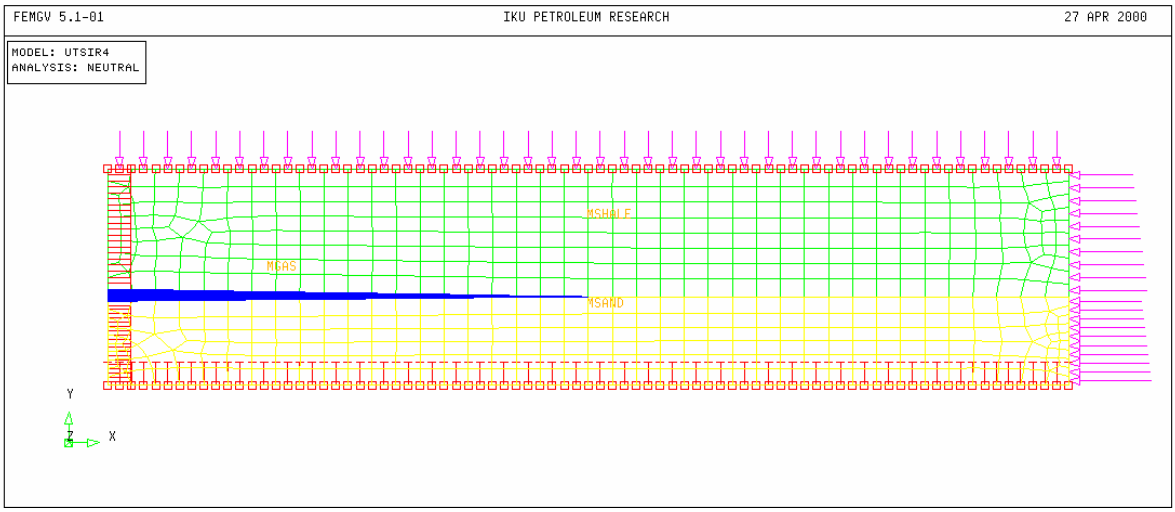

Figure 3.2 *Schematic of FEM model. The mesh consists of about 1000 elements. Lateral extension is 1600 m, vertical 360 m. The green part is the shale cap rock, the blue is the gas-filled dome region and the yellow is the sand. The model is axisymmetric about the left vertical. Purple arrows indicate loads: The load on the top surface corresponds to the gravitational load of the remaining overburden (12.6 MPa at 680 mMD), while the load on the right end surface is the horizontal stress (around 9-10 MPa, increasing linearly with depth in each region). The loads are adapted from the log in well 15/9-C-2H (EXLOG Drillbyte EAP: OBG Data, well path 15/9-C-2H). Gravitational load is applied. Mechanical parameters are as tabulated in Table 3.3. Red squares mark constant pore pressures (here fixed at bottom and top of model). Horizontal (vertical) T-bars mark where horizontal (vertical) displacement is constrained to zero.*

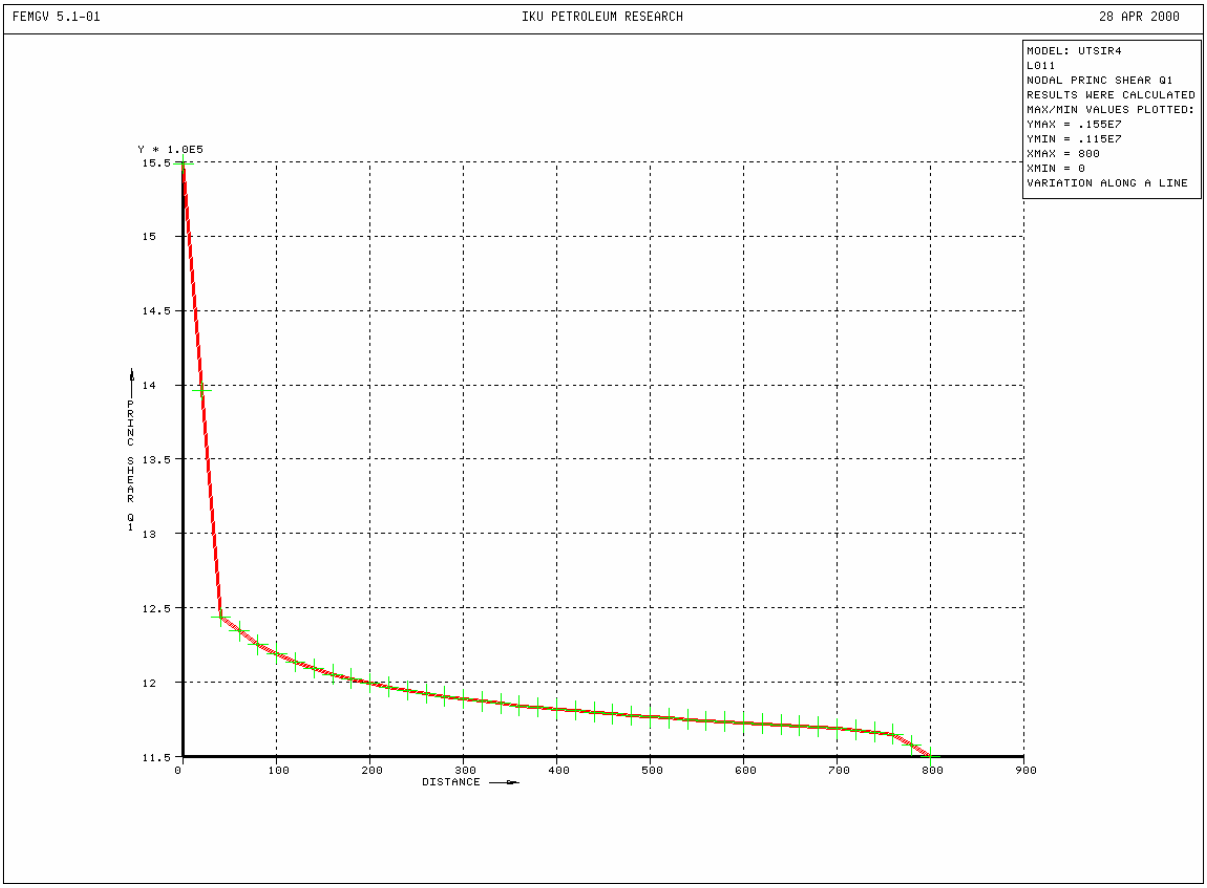

Figure 3.3 *Maximum principal shear stress along the gas/cap rock interface from the centre to the end. Stresses in Pascals, distances in meters. Note that due to the sharp mathematical wedge shapes of the dome (gas) region at the top (corresponding to a distance of 0) and at the right (at 800 m distance), we expect numerical artefacts there, here manifested as peaks close to distances 0 and 800 m. The maximum shear stress is moderate, and no Mohr-Coulomb failure results, as explicitly presented Figure 3.4 below.*

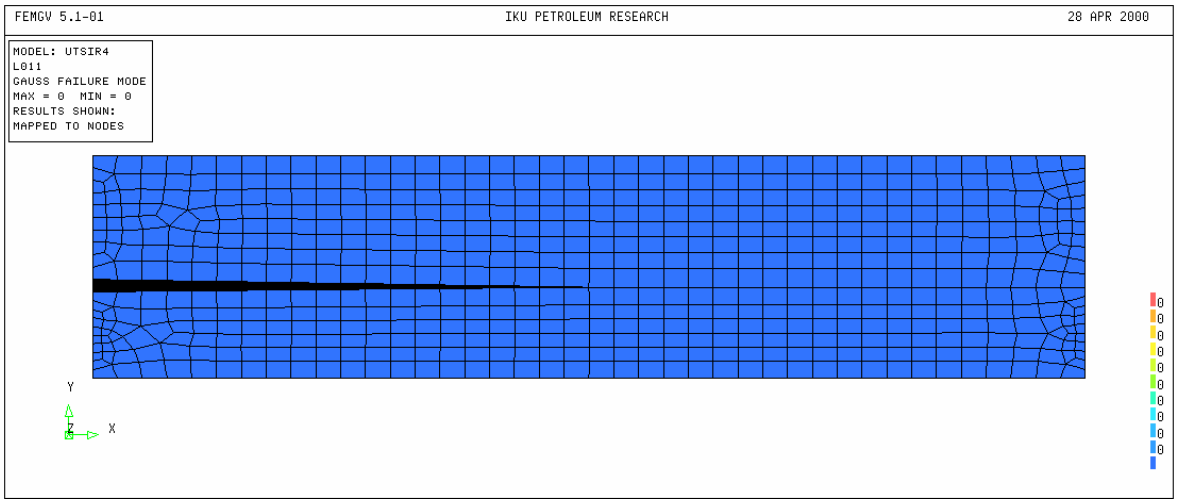

Figure 3.4 Mohr-Coulomb failure results, where a failure mode value of 0 means no failure.

3.6 Conclusions

From the numerical considerations of Sections 3.3 to 3.5 above, mechanical failure of the cap rock is not likely.

4. References

Brudy, M., 1998: Determination of the state of stress by analysis of drilling-induced fractures – results from the Northern North Sea. EUROCK98, SPE/ISRM-conference Rock Mechanics in Petroleum Engineering, Trondheim, 8-10 July 1998, Proceedings, p. 141-149 (SPE/ISRM paper 47236).

Brudy, M. & Kjørholt, H., 2001: Stress orientation on the Norwegian continental shelf derived from borehole failures observed in high-resolution borehole imaging logs. Tectonophysics, 337, 65-84.

Brudy, M., Zoback, M.D., Fuchs, K., Rummel, F. and Baumgaertner, J., 1997: Estimation of the complete stress tensor to 8km depth in the KTB scientific drill holes: Implications for crustal strength. Journal of Geophysical Research, 102, (B8), p. 18453-18575.

Bøe, R. & Zweigel, P., 2001: Characterisation of the Nordland Shale by XRD analysis- A contribution to the Saline Aquifer CO2 Storage (SACS) project. SINTEF Petroleum Research report 33.0764.00/01/01, 23 p., confidential.

Cartwright, J.A. & Lonergan, L., 1996: Volumetric contraction during the compaction of mudrocks: a mechanism for the development of regional-scale polygonal fault systems. Basin Research, 8, 183-193.

Cloething, S., Gradstein, F.M., Kooi, H., Grant, A.C. and Kaminski, M., 1990: Plate reorganization: a cause of rapid late Neogene subsidence and sedimentation around the North Atlantic? Journal of the Geological Society of London, 147, p. 495-506.

Cloething, S., Reemst, P., Kooi, H. and Fanavoll, S., 1992: Intraplate stresses and the post-Cretaceous uplift and subsidence in northern Atlantic basins. Norsk Geologisk Tidsskrift, 72, p. 229-235.

Cowgill, S.M., Meredith, P.G., Murrell, S.A.F. and Brereton, N.R., 1995: The orientation of stress-induced wellbore breakouts in the North Sea Basin – a case study. In: Workshop on rock stresses in the North Sea, Trondheim, 13-14 February 1995, Proceedings, p.202- 217.

Dewhurst, D.N., Cartwright, J.A. and Lonergan, L., 1999: The development of polygonal fault systems by syneresis of colloidal sediments. Marine and Petroleum Geology, 16, 793-810.

Eidvin, T., Riis, F. and Rundberg, Y., 1999: Upper Cainozoic stratigraphy in the central North Sea (Ekofisk and Sleipner fields). Norsk Geologisk Tidsskrift, 79, 97-128.

Fejerskov, M. and Bratli, R, 1998: Can dipmeter logs be used to identify in-situ stress directions in the North Sea? EUROCK98, SPE/ISRM-conference Rock Mechanics in Petroleum Engineering, Trondheim, 8-10 July 1998, Proceedings, p. 151-160 (SPE/ISRM paper 47237).

Fejerskov, M., 1996: Determination of in-situ rock stresses related to petroleum activities on the Norwegian continental shelf. PhD thesis, NTNU Trondheim, 162 pp + Appendix.

Fejerskov, M., Myrvang, A.M., Lindholm, C. and Bungim, H., 1995: In-situ rock stress pattern on the Norwegian continental shelf and mainland. In: Workshop on rock stresses in the North Sea, Trondheim, 13-14 February 1995, Proceedings, p. 191-201.

Fejerskov, M. & Lindholm, C., 2000: Crustal stress in and around Norway: an evaluation of stress-generating mechanisms. In: Nøttvedt, A. et al. (eds.): Dynamics of the Norwegian Margin. Geol. Soc. Spec. Publ., 167, 451-467.

Fejerskov, M., Lindholm, C., Myrvang, A. & Bungum, H., 2000: Crustal stress in and around Norway: a compilation of *in situ* stress obeservations. In: Nøttvedt, A. et al. (eds.): Dynamics of the Norwegian Margin. Geol. Soc. Spec. Publ., 167, 441-449.

Gabrielsen, R.H., Odinsen, T., Grunnaleite, I. 1999: Structuring of the Northern Viking Graben and the Møre Basin; the influence of basement structural grain, and the particular role of the Møre-Trøndelag Fault Complex. Marine and Petroleum Geology, v. 16(5), p. 443-465.

Goelke, M. and Brudy, M., 1996: Orientation of crustal stresses in the North Sea and Barents Sea inferred from borehole breakouts. Tectonophysics, 266, p. 25-32.

Goelke, M., 1996: Patterns of stress in sedimentary basins and the dynamics of pull-apart basin formation. PhD thesis, Vrije Universiteit Amsterdam, 167 pp.

Gradstein, F.M., Kaminski, M.A., Berggren, W.A., Kristiansen, I.L. and D'Iorio, M.A., 1994: Cenozoic biostratigraphy of the North Sea and Labrador Shelf. Micropaleontology, 40, supplement, p. 1 – 152.

Gregersen, S. 1992: Crustal, stress regime in Fennoscandia from focal mechanisms. Journal of Geophysical Research, vol. 97, (B8), p. 11,821-11,827.

Gregersen, S., Korhonen, H., and Husebye, E.S., 1991: Fennoscandian dynamics: Present-day earthquake activity. Tectonophysics, 189, p. 333-344.

Grollimund, B., Zoback, M.D., Wiprut, D.J., & Arnesen, L., 2001: Stress orientaton, pore pressure and least principal stress in the Norwegian sector of the North Sea. Petroleum Geoscience, 7, 173-180.

Grollimund, B. & Zoback, M.D., 2000: Post glacial lithospheric flexure and induced stresses and pore pressure changes in the northern North Sea. Tectonophysics, 327, 61-81.

Holloway et al. 2000: Final report of the SACS 1 project – Saline Aquifer CO2 Storage: A demonstration at the Sleipner Field. Work Area 1 – Geology. BGS Technical Report WH/2000/21C (Confidential).

Jørgensen, T. and Bratli, R.K., 1995: In-situ stress determination and evaluation at the Tampen Spur area. In: Workshop on rock stresses in the North Sea, Trondheim, 13-14 February 1995, Proceedings, p. 240-249.

Kooi, H., Hettema, M. and Cloething, S., 1991: Lithospheric dynamics and the rapid Pliocene-Quaternary subsidence phase in the southern North Sea basin. Tectonophysics, 192, p. 245-259.

Lindholm, C.D., Bungum, H., Villagran, M., and Hicks, E., 1995b: Crustal stress and tectonics in Norwegian regions determined from earthquake focal mechanisms. In: Workshop on rock stresses in the North Sea, Trondheim, 13-14 February 1995, Proceedings, p. 77-91.

Lindholm, C.D.; Bungum, H.; Bratli, R.K.; Aadnøy, B.S.; Dahl, N.; Tørudbakken, B.; & Atakan, K. 1995: Crustal Stress in the northern North Sea as inferred from borehole breakouts and earthquake focal mechanisms. Terra Nova 7, 51-59.

Lindholm, C.D., Bungum, H., Hicks, E., & Villagran, M., 2000: Crustal stress and tectonics in Norwegian regions determined from earthquake focal mechanisms. In: Nøttvedt, A. et al. (eds.): Dynamics of the Norwegian Margin. Geol. Soc. Spec. Publ., 167, 429-439.

Lothe, A.E. and Zweigel, P., 1999: Saline Aquifer CO2 Storage (SACS) – Informal annual report 1999 of SINTEF Petroleum Research's results in work area 1 "Reservoir Geology". SINTEF Petroleum Research report 23.4300.00/03/99, 54 pp. + appendix.

Mueller, B., Wehrle, V., and Fuchs, K. (1997): The 1997 release of the World Stress Map (available on-line at http://www-wsm.physik.uni-karlsruhe.de/pub/Rel97/wsm97.html)

Pascal, C. & Gabrielsen, R. ,1999: Numerical modelling of Cenozoic strain/stress patterns and fault slip restoration in the mid-Norwegian margin and the northern North Sea. Chapter 16 in: Gabrielsen et al.: Tectonic impact on sedimentary processes in the post-rift phase – Improved models. SINTEF Petroleum Research report 23.2661.00/01/99, 30 pp.

Pascal, C. & Gabrielsen, R.H., 2001: Numerical modeling of Cenozoic stress patterns in the mid-Norwegian margin and the northern North Sea. Tectonics, 20 , 585-599.

Pascal, C., Gabrielsen, R., Zweigel, P., Saettem, J. and Angelier, J., 1999: Prediction of Late Cenozoic fault reactivation in the northern North Sea and the Mid-Norwegian Margin from numerical simulations of far-field stress effects. Winter meeting of Norsk Geologisk Forening, Stavanger, January 1999, Proceedings (Geonytt 1/99), p. 80-81.

Spann, H., Mueller, B. and Fuchs, K., 1991: Interpretation of anomalies in observed stress data at the Central Graben (North Sea), numerical and analytical approach. Soil Dynamics and Earthquake Engineering, 13, p. 1-11.

Stephanson, O., Ljunggren, C. and Jing, L., 1991: Stress measurements and tectonic implications for Fennoscandia. Tectonophysics, 189, p. 317-322.

Underhill, J. R., and M. A. Partington, 1993, Jurassic thermal doming and deflation in the North Sea: implications of the sequence stratigraphic evidence, *in* J. R. Parker, ed., Petroleum Geology of Northwest Europe, Geological Society of London, p. 337-345.

Wiprut, D.J. and Zoback, M.D., 1998: High horizontal stress in the Visund field, Norwegian North Sea: consequences for borehole stability and sand production. EUROCK98, SPE/ISRM-conference Rock Mechanics in Petroleum Engineering, Trondheim, 8-10 July 1998, Proceedings, p. 199-208 (SPE/ISRM paper 47244).

Wiprut, D. & Zoback, M.D., 2000: Fault reactivation and fluid flow along a previously dormant normal fault in the northern North Sea. Geology, 28, 595-598.

Wood, R.J., 1981: The subsidence history of Conoco well 15/30-1, central North Sea. Earth and Planetary Science Letters, 54, p. 306-312.

Zoback, M.D., Apel, R., Baumgaertner, J., Brudy, M., Emmermann, R., Engeser, B., Fuchs, K., Kessel, W., Rischmueller, H., Rummel, F. and Vernik, L., 1993: Upper crustal strength inferred from stress measurements to 6 km depth in the KTB borehole. Nature, 365, p. 633-635.

Zoback, M.L., 1992: First and second order patterns of stress in the lithosphere. The World Stress Map project. Journal of Geophysical Research, 97, p. 11703-11728.

Aadnøy, B.S. and Berland, S., 1995: Stress modelling versus real borehole behaviour. In: Workshop on rock stresses in the North Sea, Trondheim, 13-14 February 1995, Proceedings, p. 22-37.

Appendix A Overcoring data from South-western Norway

WSM 1997-1 (Mueller et al. 1997)

Site name	Latitude	Longitude	depth [km]	S1 (MPa)	S2(Mpa)	S3(Mpa)	Quality	Azi SH	Regime	SH (Mpa)	Sh (Mpa)	SV (Mpa)	s1-s3	s1 / s3	sH / Sh
NW 18	60.600	4.733	0.111	8.6	5.1	2.4	D	179	SS	7.9	2.5	5.1	6.2	3.6	3.2
NW 19	60.817	5.033	0.075	6.8	3.8	2.5	D	173	SS	6.8	2.5	3.8	4.3	2.7	2.7
NW 20	61.217	6.083	0.63	29.5	19	14.1	D	40	SS	29.4	14.7	19	15.4	2.1	2
NW 21	60.067	6.550	0.185	6.7	1.7	0.6	D	139	NF	3.5	0.6	6.7	6.1	11.2	5.8
NW 22	60.850	7.100	0.725	31.8	27.5	17.6	D	88	SS	31.3	18.1	27.5	14.2	1.8	1.7
NW 23	60.500	7.133	0.475	19.5	9.5	4.8	D	127	NF	9.7	5.1	19.5	14.7	4.1	1.9
NW 24	61.517	7.300	0.443	16.7	14.6	3.7	B	101	TF	16.9	11.4	3.7	13	4.5	1.5
NW 25	61.200	7.617	0.675	26.3	19.6	16.8	D	116	NF	17.3	13	26.3	9.5	1.6	1.3
NW 28	58.317	6.383	0.075	4.5	3.9	2.3	D	20	TF	5.6	4.2	2.3	2.2	2	1.3
NW 43	60.133	6.333	0.48	24.5	13	0.5	E	102	U	19.2	6.5		24	49	3
NW 44	61.400	6.750	0.375	26.2	14.9	6.6	D	38	TS	25.6	11.8	*6.6*	19.6	4	2.2
												mean:	**11.7**		

Fejerskov (1996)

Site name	Latitude	Longitude	depth [km]	S1 (MPa)	S2(Mpa)	S3(Mpa)	Quality	Azi SH	Regime	SH (Mpa)	Sh (Mpa)	SV (Mpa)	s1-s3	s1 / s3	sH / Sh
Hjartøy01	60.600	4.789	0	1	-0.4	-3.8	C	3	SS	0.5	-3.8	0.1	4.8	-0.3	-0.1
Hjartøy02	60.600	4.789	0	3.3	-1.1	-3.7	D	88	NF	-1.1	-3.4	2.9	7	-0.9	0.3
Hjartøy03	60.600	4.789	0	5.8	2	1.4	C	41	TF	5.6	2	1.6	4.4	4.1	2.8
Jøssingfjord01	58.305	6.333	0.3	13	7.9	3.5	C	148	TF	12.5	5.7	6.2	9.5	3.7	2.2
Kvilldal01	59.018	6.638	0.3	12.2	8.5	4.3	C	67	NF	9.8	4.9	10.3	7.9	2.8	2
Kvilldal02	59.018	6.638	0.3	9.9	7.1	5.2	A	94	NF	7.7	5.3	9.3	4.7	1.9	1.5
Lysefjorden01	59.050	6.653	0.65	21.6	7.4	5.7	D	97	NF	7.4	5.7	21.6	15.9	3.8	1.3
Mauranger02	60.129	6.323	0.3	37.3	19.8	-5	C	159	NF	12.7	10.4	20.1	42.3	-7.5	1.2
Odda01	60.061	6.553	0.185	8.1	3.8	2.1	D	143	NF	5.4	2.2	6.4	6	3.9	2.5
Sture01	60.618	4.833	0.09	1.5	0.9	-0.7	B	84	SS	1.5	-0.4	0.6	2.2	-2.1	-3.8
Sture02	60.618	4.833	0.05	2.3	0.1	-1.7	C	49	TF	2.1	-0.5	-1	4	-1.4	-4.2
Titania01	58.344	6.428	0.05	7.1	4.7	3.9	C	165	SS	7.1	4.2	4.4	3.2	1.8	1.7
Titania02	58.344	6.428	0.1	5	4.5	2.4	C	25	TF	4.7	4.5	2.7	2.6	2.1	1
												mean:	**8.8**		
												mean all:	**10.4**		
												std dev	**9**		
												median:	**7.9**		

S1, S2, S3: Magnitudes of principal stresses (S1>S2>S3, compression being positive); Azi SH: Azimuth of S_H; Regime: SS = strike-slip, TF = thrust faulting, TS = oblique thrust faulting, NF = normal faulting, NS = oblique normal faulting; SH: Magnitude of maximum horizontal stress; Sh: magnitude of minimum horizontal stress; SV: magnitude of vertical stress.